Cenozoic Stratigraphy

http://www.flickr.com/photos/41427631@N03/4790121151/in/photostream


APAT
Agenzia per la Protezione dell'Ambiente e per i Servizi Tecnici
Dipartimento Difesa del Suolo
Servizio Geologico d'Italia
GEOLOGICAL MAP OF ITALY
1:1 250 000 Scale
MAIN TECTONO-STRATIGRAPHIC UNITS
OFFICIALLY PRINTED FOR THE 32nd INTERNATIONAL GEOLOGICAL CONGRESS
ITALIA 2004

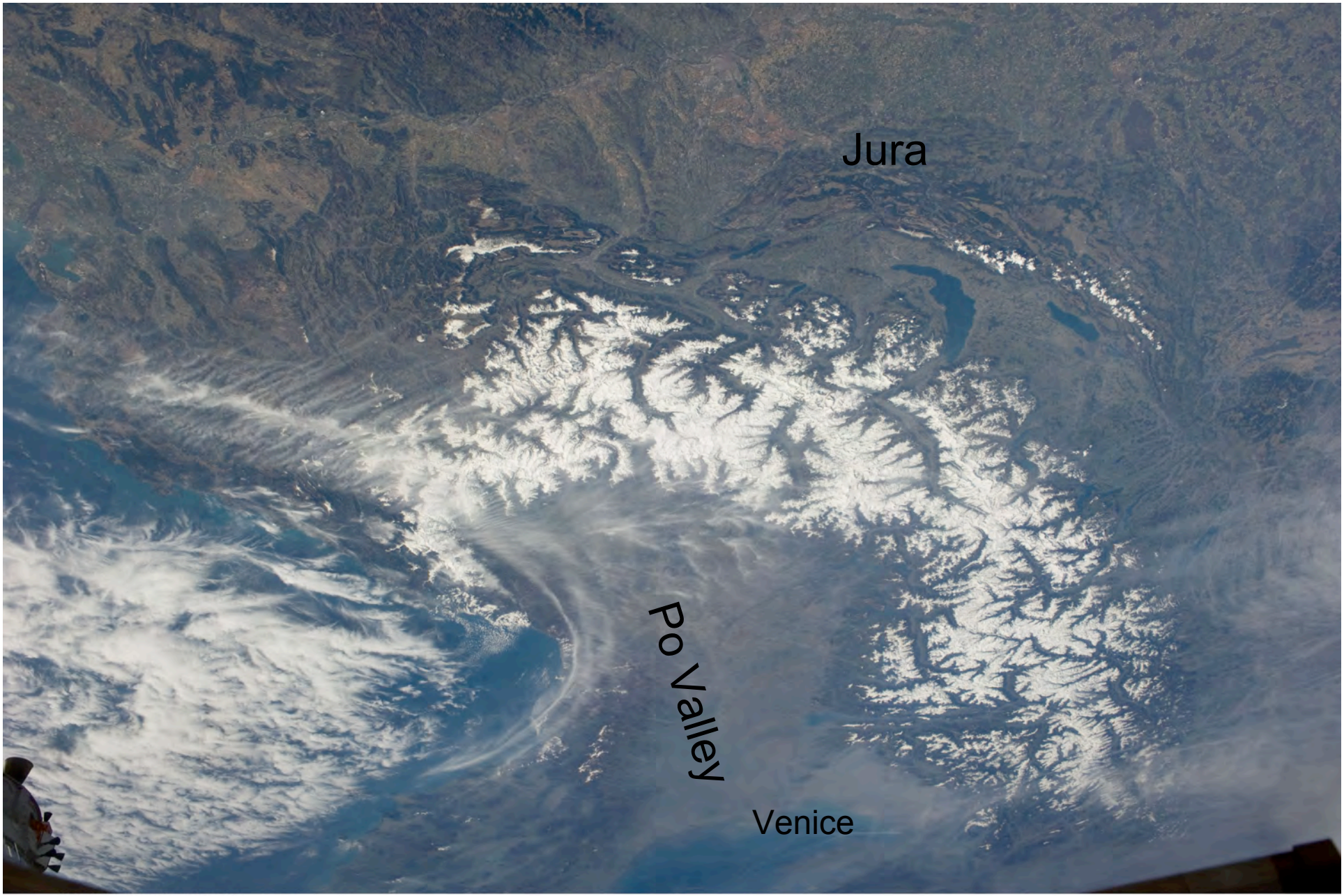

ISS027E007723

Alps, Lake Geneva, Adriatic

http://eol.jsc.nasa.gov/

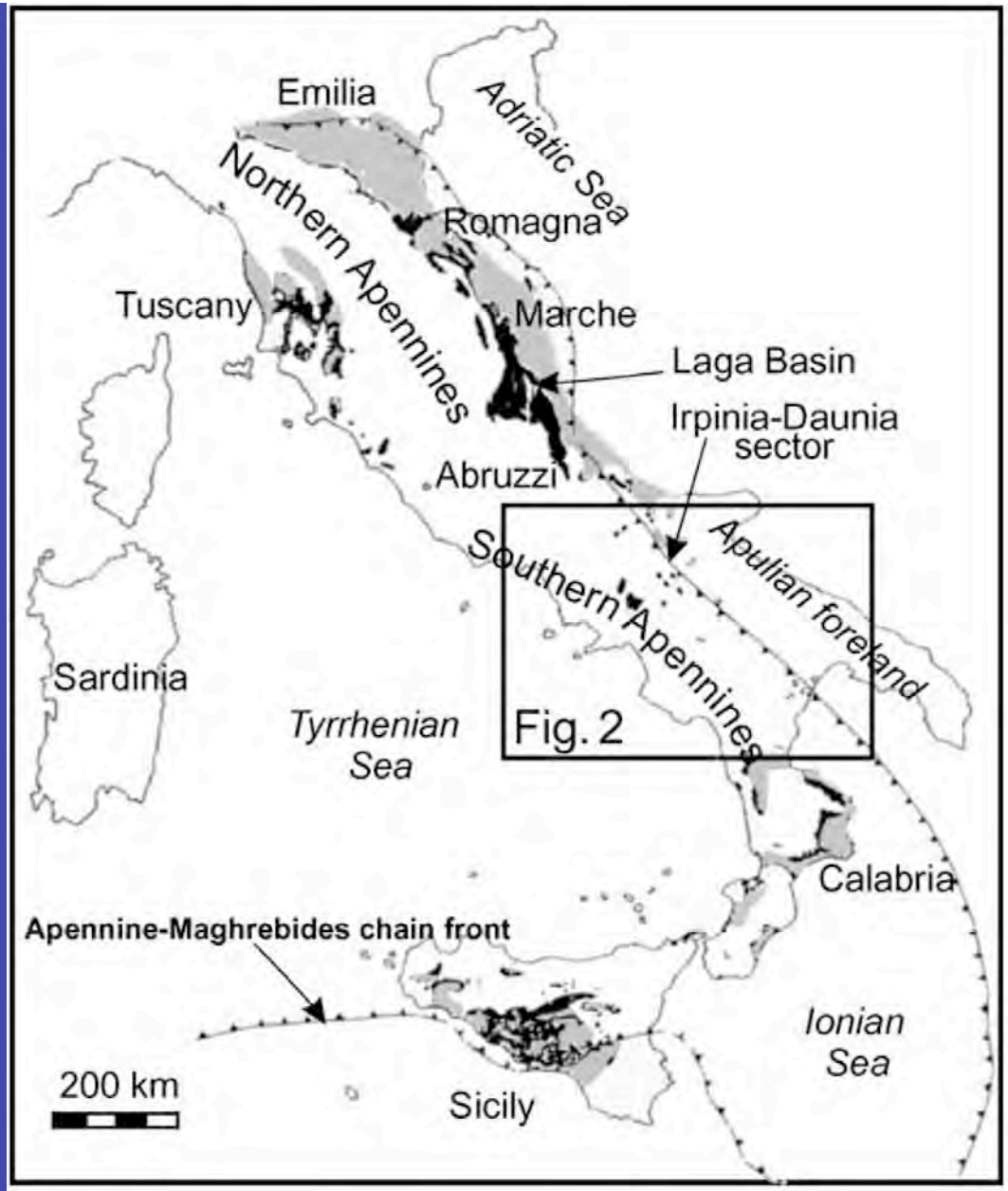

Fig. 1. Distribution of Messinian deposits (black: outcrops; gray: buried deposits) within peninsular Italy and Sicily (modified after Selli, 1973 and Roveri et al., 2001).

Matano et al 2005

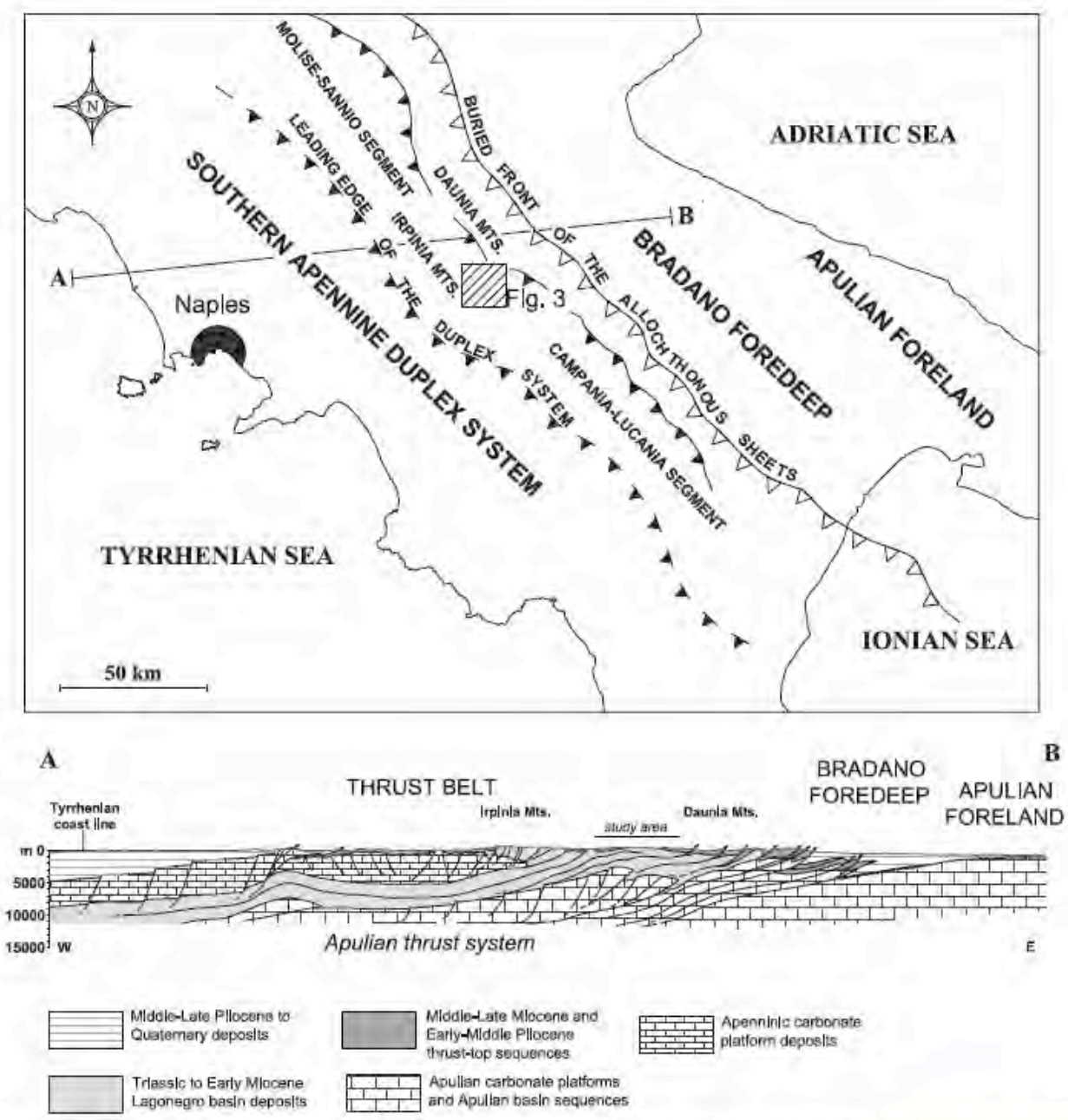

Fig. 2. Southern Apennines tectonic scketch-map with simplified geological section (modified after Mostardini and Merlini, 1986).

Matano et al 2005

Digression: deposition of evaporite rocks and minerals

Great Salt Lake: internally Drained basin

Trucial coast (UAE) sabhka salt Pans on margin of Arabian Sea

Two modern evaporite environments

Evaporite Deposition Model

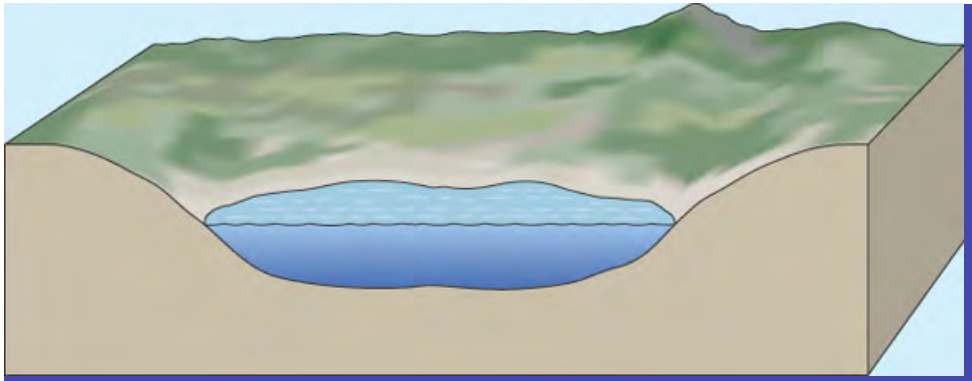

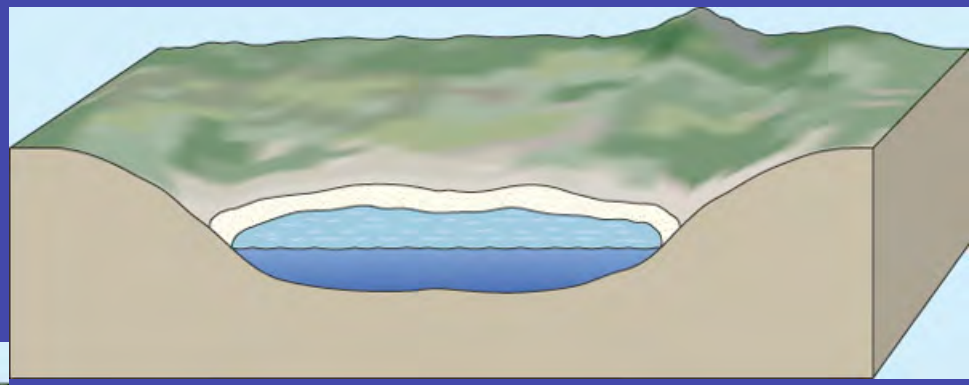

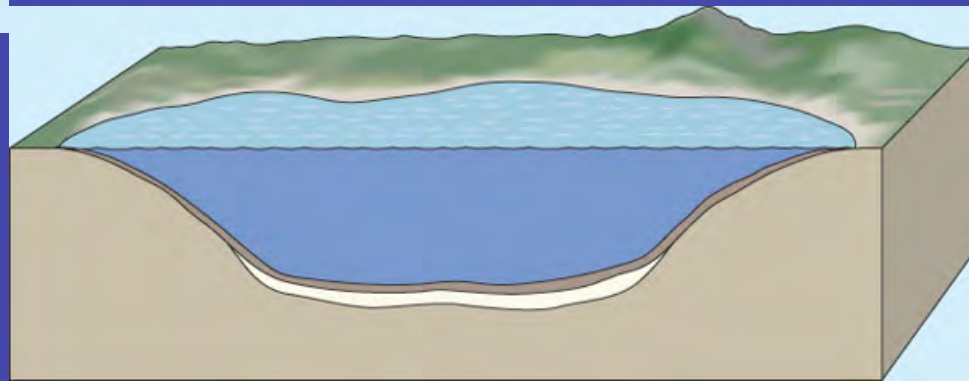

http://www.divediscover.whoi.edu/dhabs/geology.html

Gypsum

Anhydrite

Halite

Calcite

http://geology.com/minerals/

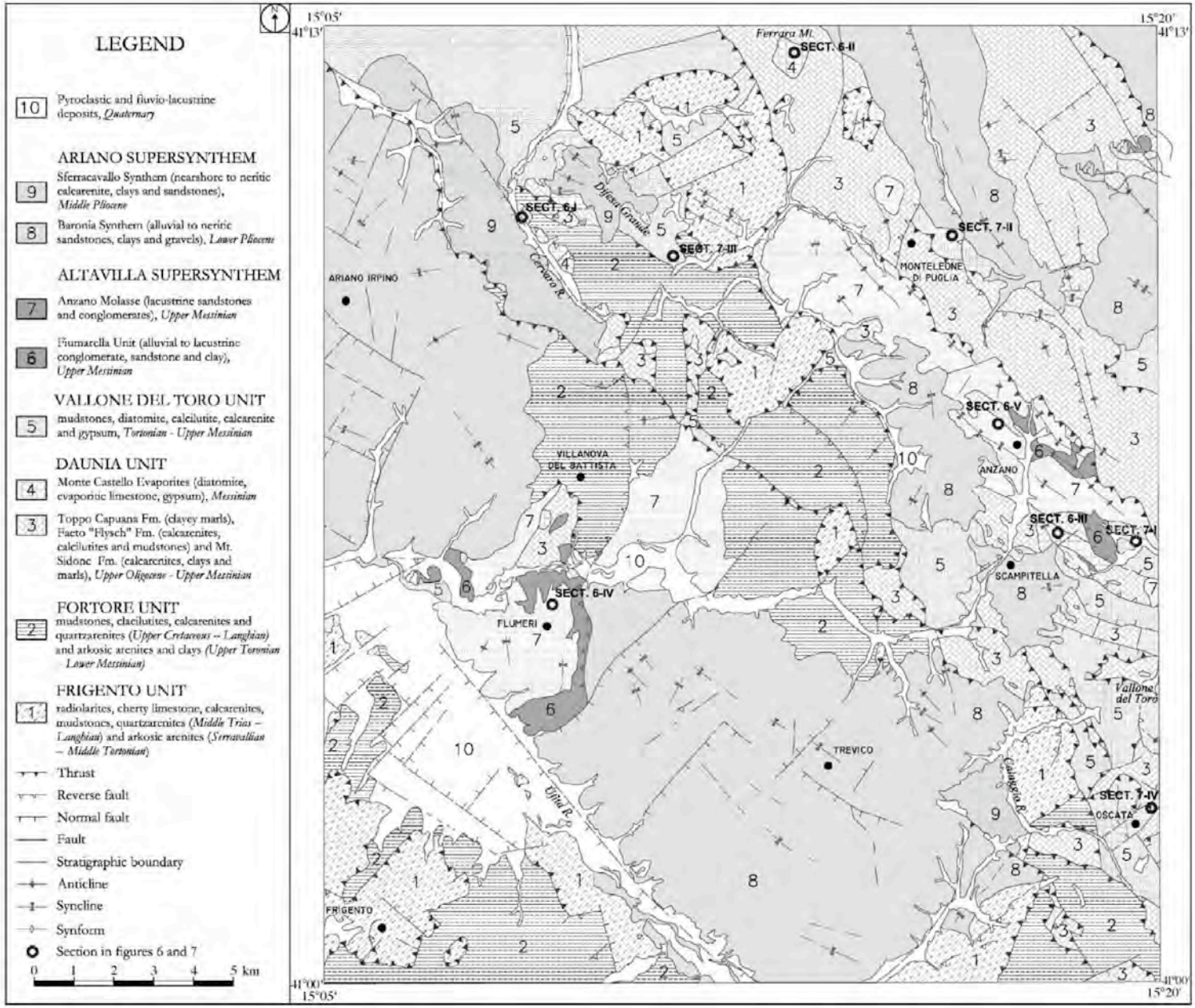

g. 3. Geological map of the Irpinia-southern Daunia Mt. sector of southern Apennines (Italy). The numbers in the section labels refers to figure and column in which the section is owed. Area location is indicated in Fig. 2.

Matano et al 2005

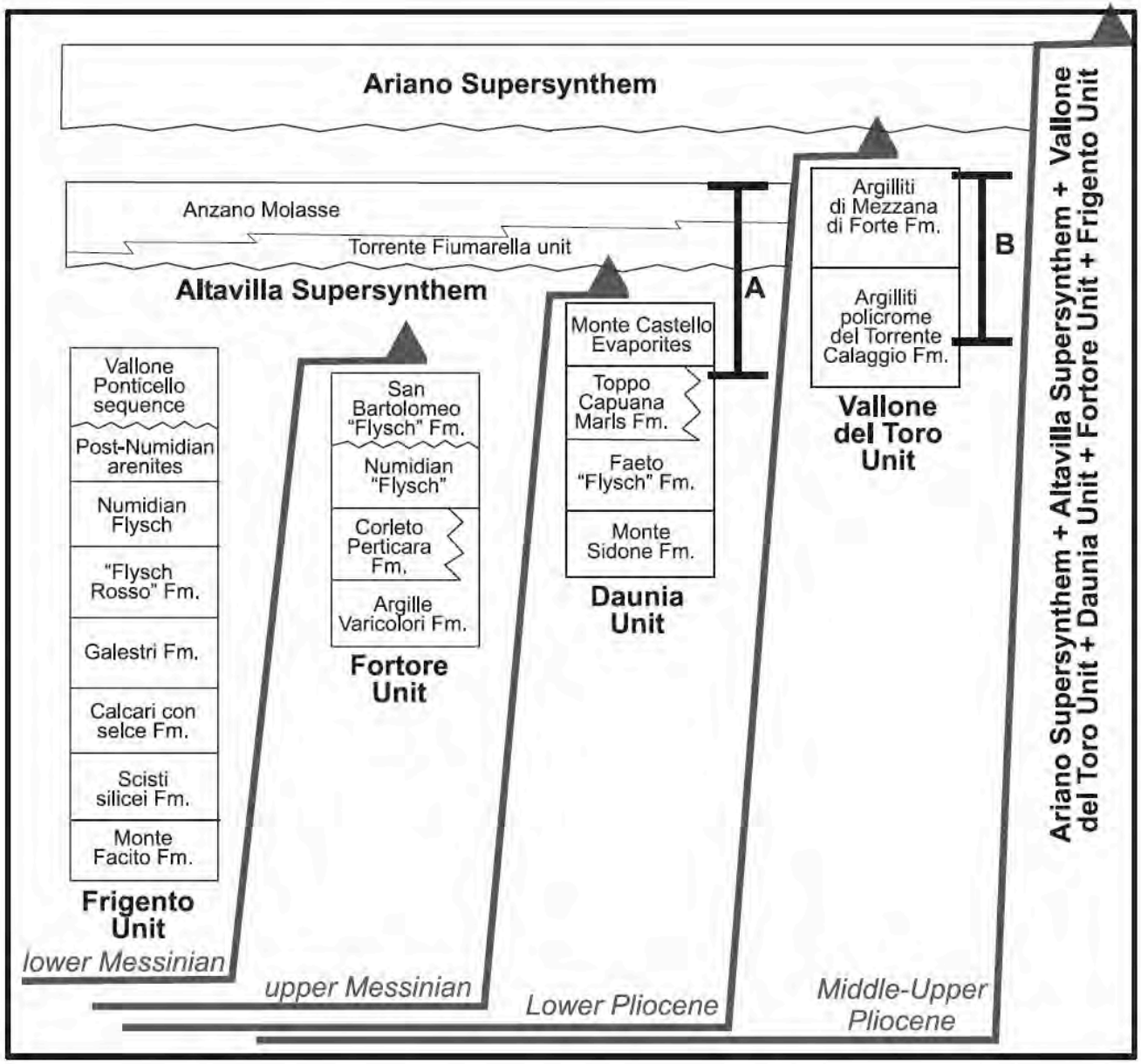

g. 4. Tectonic and stratigraphic scheme of the main units cropping out in the Irpinia-Daunia Mts. Legend: A, unit A; B, unit B; black line with angle, thrust slices (at the foot of the lines the age of thrusting is given).

Matano et al 2005

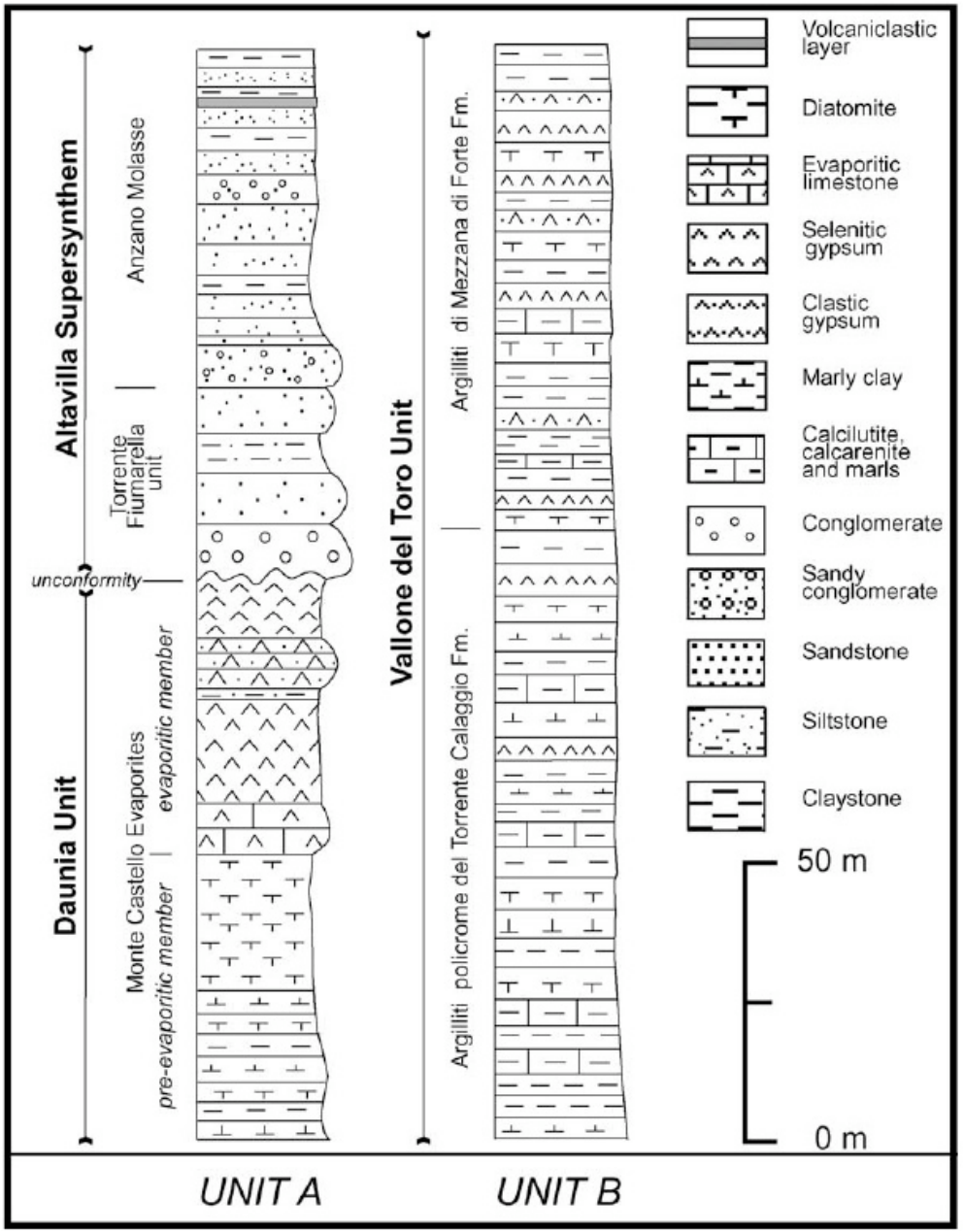

Fig. 5. Stratigraphic synthetic logs of the Messinian successions cropping out in the Irpinia-Daunia Mts.

Matano et al 2005

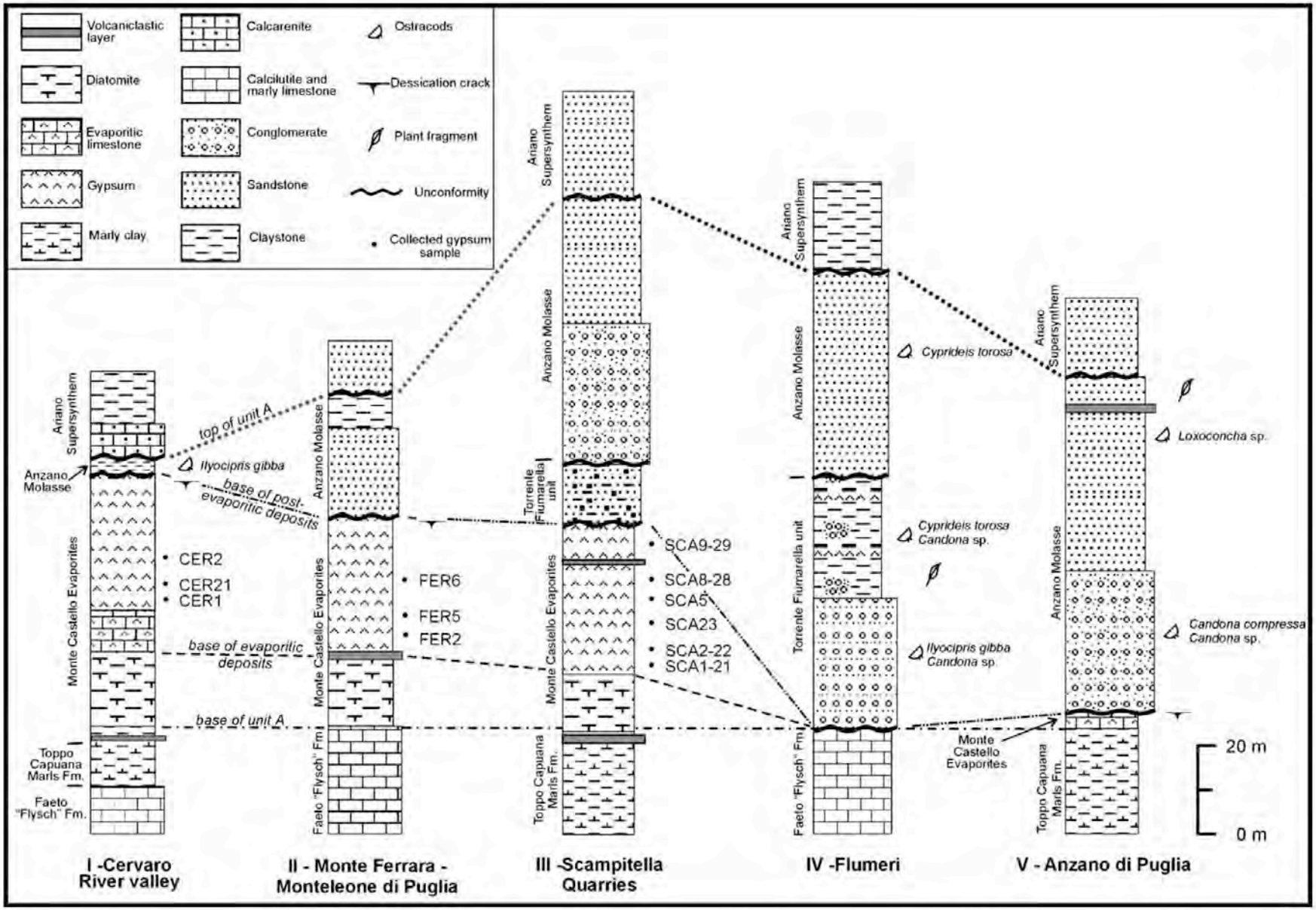

Fig. 6. Stratigraphical representative columns of the unit A. The location of the sections is indicated in Fig. 3.

Matano et al 2005

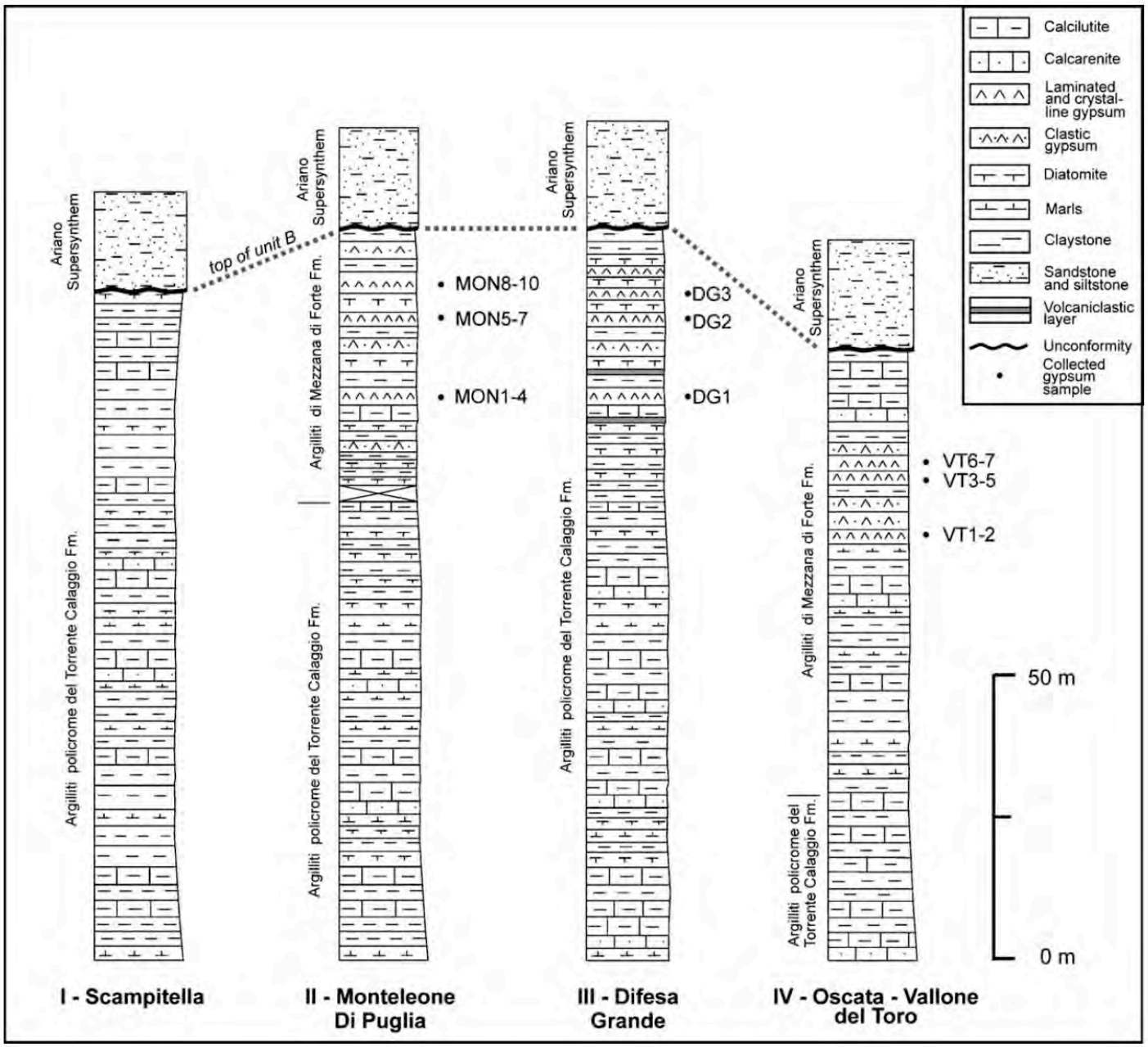

Fig. 7. Stratigraphical representative columns of the unit B. The location of the sections is indicated in Fig. 3.

Matano et al 2005

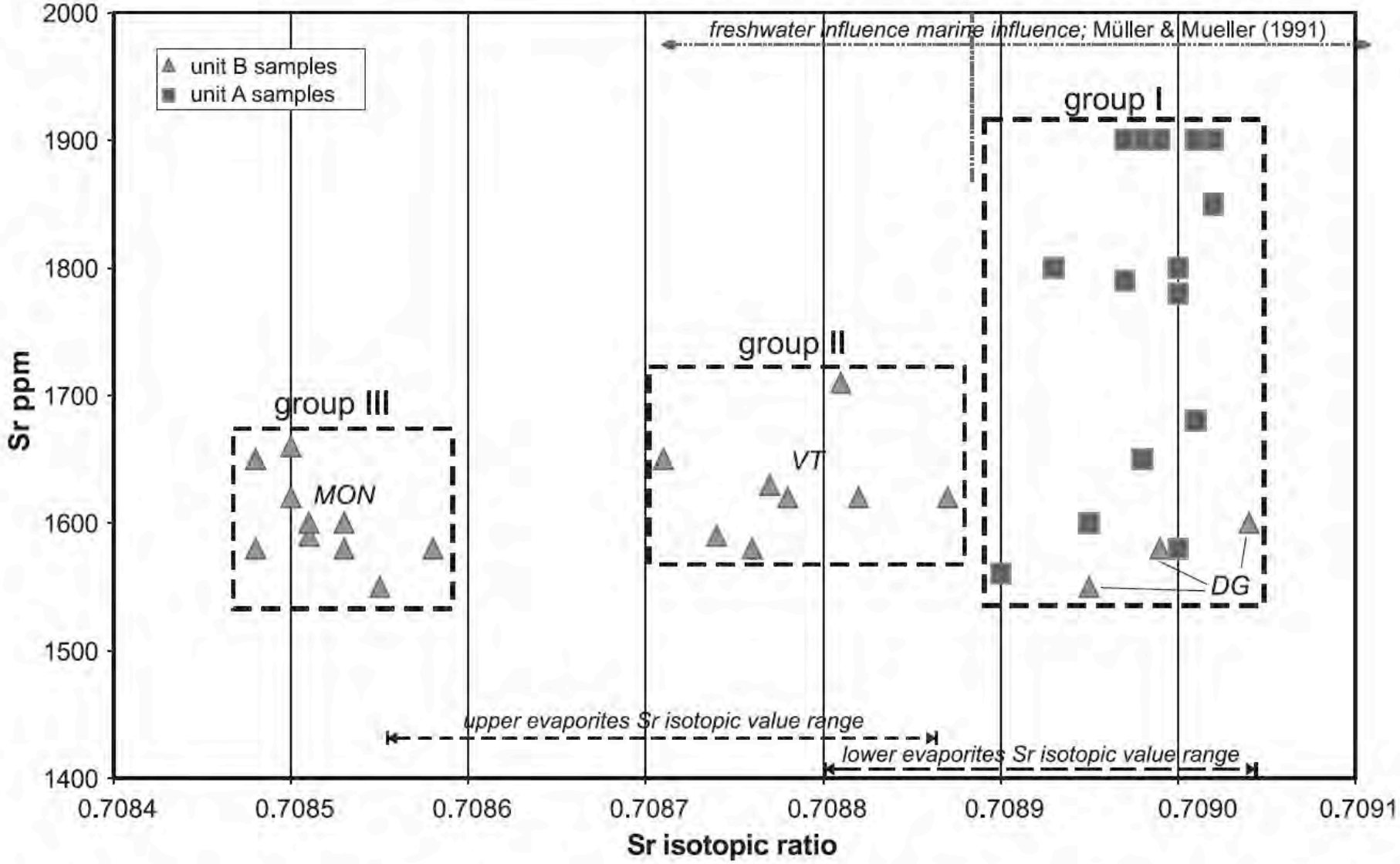

Fig. 9. Relathionships between Sr content and $^{87}Sr/^{86}Sr$ isotopic ratio of the gypsum samples and their classification. The strontium isotopic cumulative value range bars for lower and upper evaporites are derived from data in Table 1.

Matano et al 2005

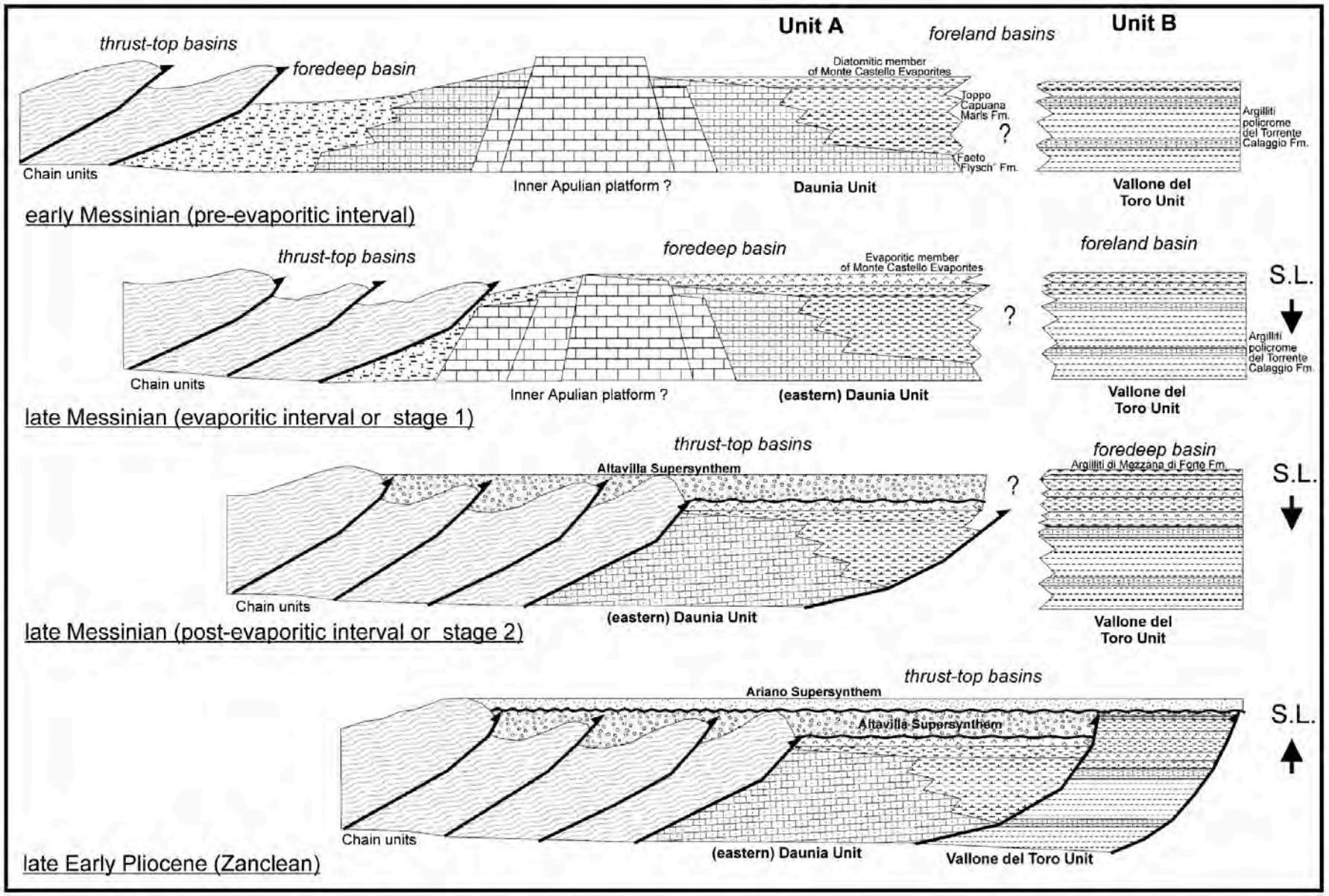

Fig. 10. Model of Messinian tectonic and stratigraphic events in the northern sector of the southern Apennine foreland basin system. For lithological patterns see Figs. 6 and 7. Arrows show sea-level trends.

Matano et al 2005

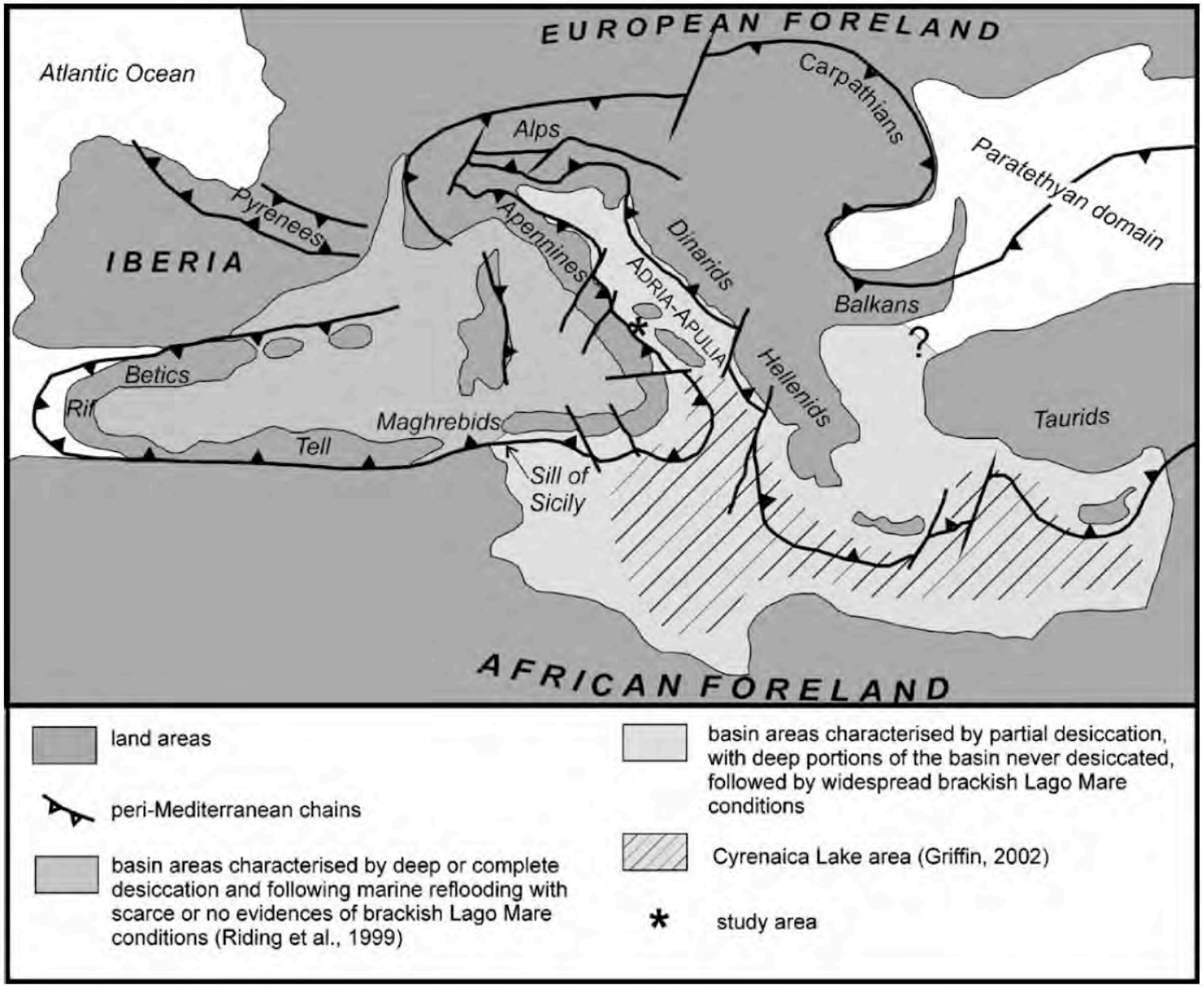

Fig. 11. Paleogeographic reconstruction of the Mediterranean domains during the late Messinian. Land areas and main thrusts distribution are from Cipollari et al. (1999a,b) and Ziegler (1999); the Mediterranean basin subdivision has been made following Riding et al. (1999, and references therein), Roveri et al. (2001), and Griffin (2002).

Matano et al 2005

Butler et al 1995

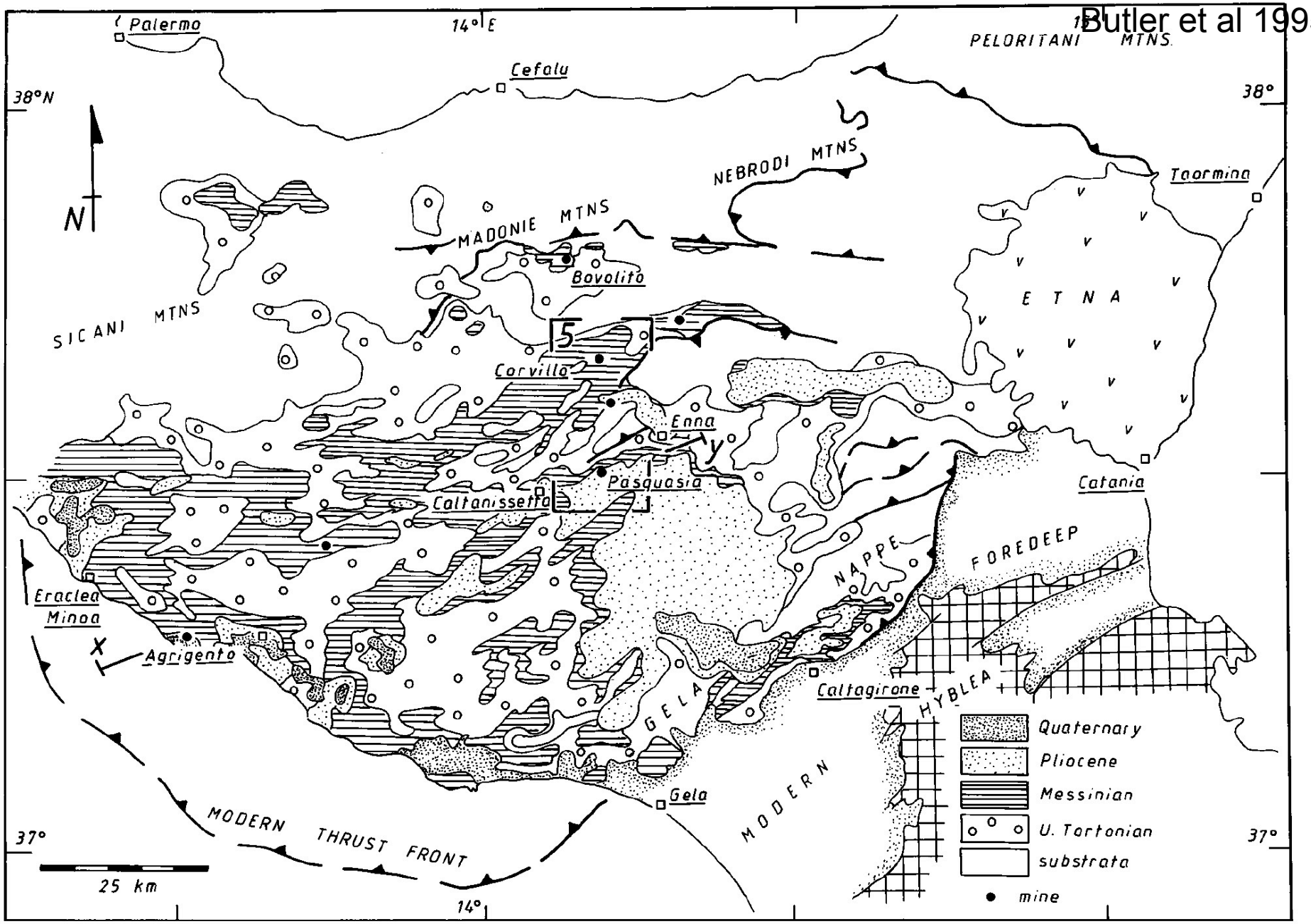

Figure 2. Geological sketch map of central Sicily showing the surface distribution of Messinian deposits and the principal mines that ploit the evaporites. The geology along the north coast is not shown. The boxed area is that covered by Figure 5. x–y is the line of the

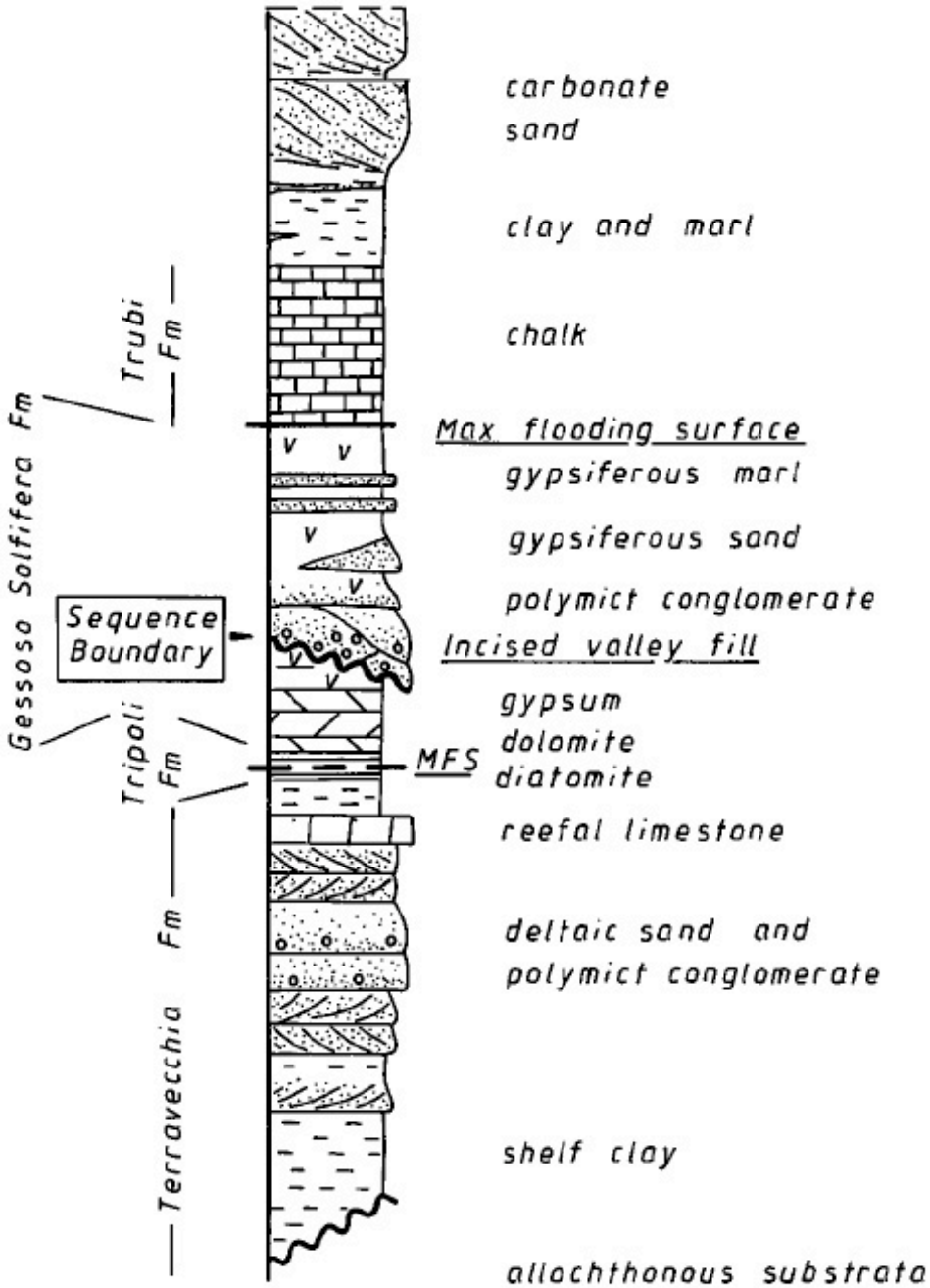

Figure 3. Lithostratigraphy for the northern part of the Caltanisetta basin (after Butler and Grasso, 1993). MFS maximum flooding surface.

Butler et al 1995

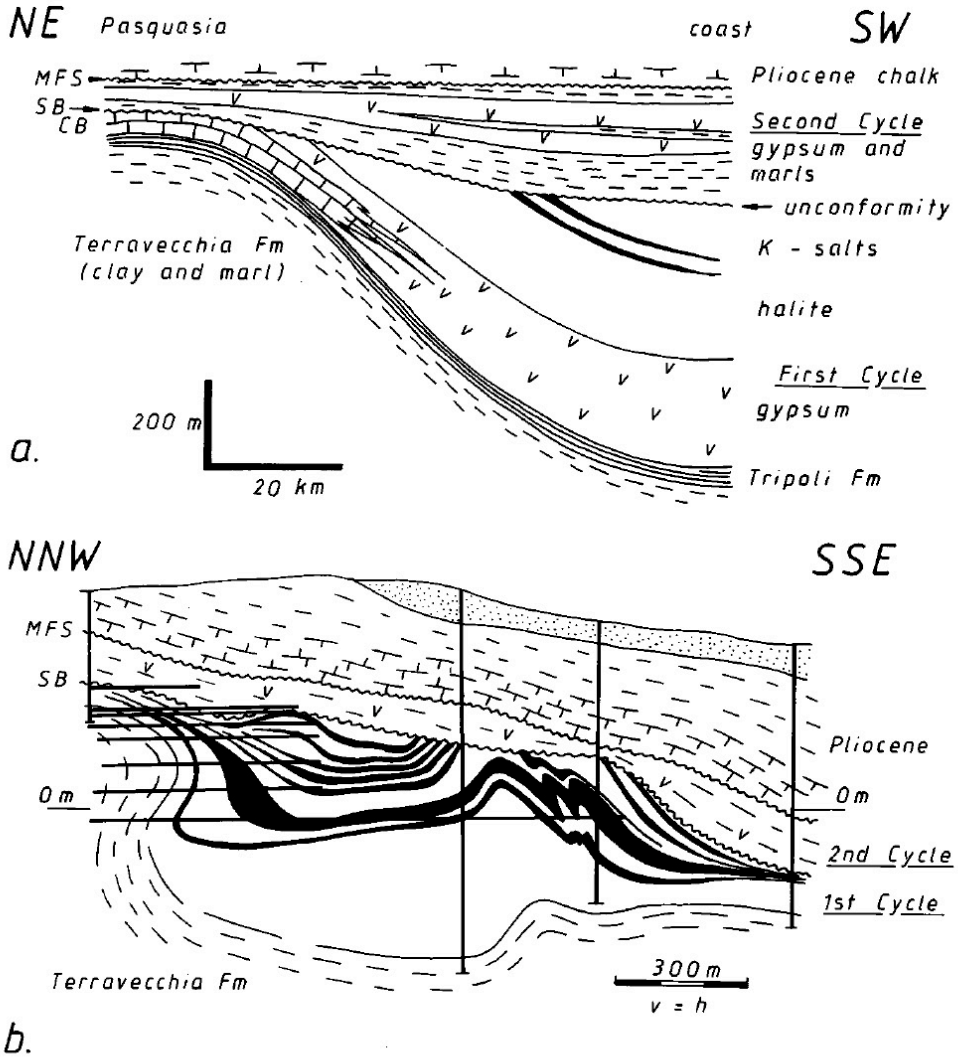

Figure 4. Scales of variations of evaporite facies and thickness within the Gessoso Solfifera Formation across the Caltanissetta basin (Locations are on Fig. 2). (a) Basinwide variations, as reported by Decima and Wezel (1973; see also Decima et al., 1988), projected onto a single northeast-southwest section line. Note the vertical exaggeration. Sequence stratigraphic interpretation is added by the present authors. CB Calcare di Base Member, MFS maximum flooding surface, SB sequence boundary. (b) True-scale cross section through Pasquasia Mine, on a north-northwest–south-southeast profile, with the same ornament and abbreviations as Figure 4a. The locations of boreholes and mine tunnels are illustrated, with no projection. The evaporites continue to crop out to the north-northwest of section where they are represented by a few meters of the Calcare di Base Member (see Fig. 4a).

Butler et al 1995

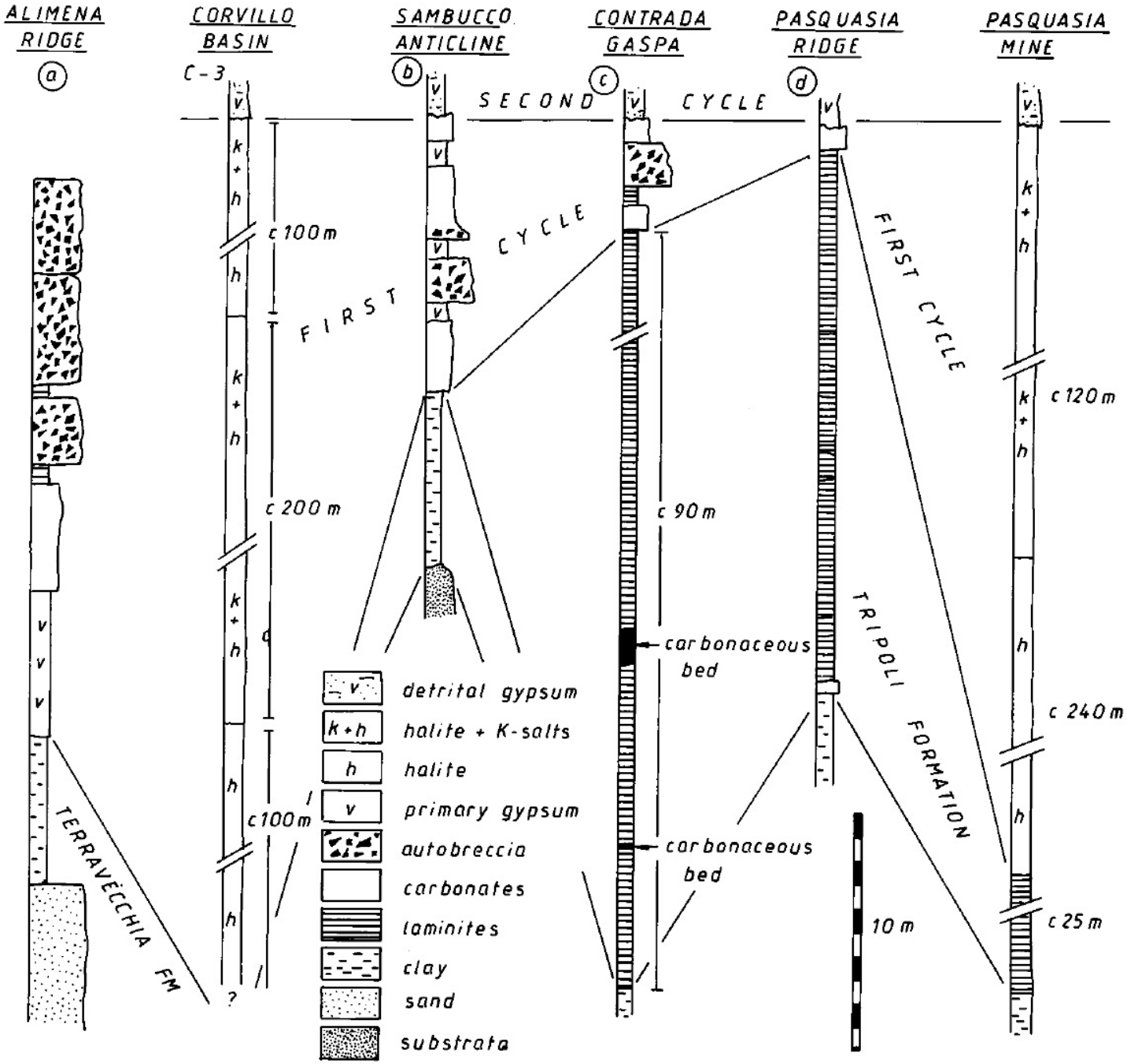

Figure 7. Measured sec through the lower trans into first cycle evapo across the northcen Caltanissetta basin, base outcrop data (Pedley Grasso, 1993) and well rec The locations of outcrop tions (a–d) and Pasqu mine (borehole) are show Figure 5.

Butler et al 1995

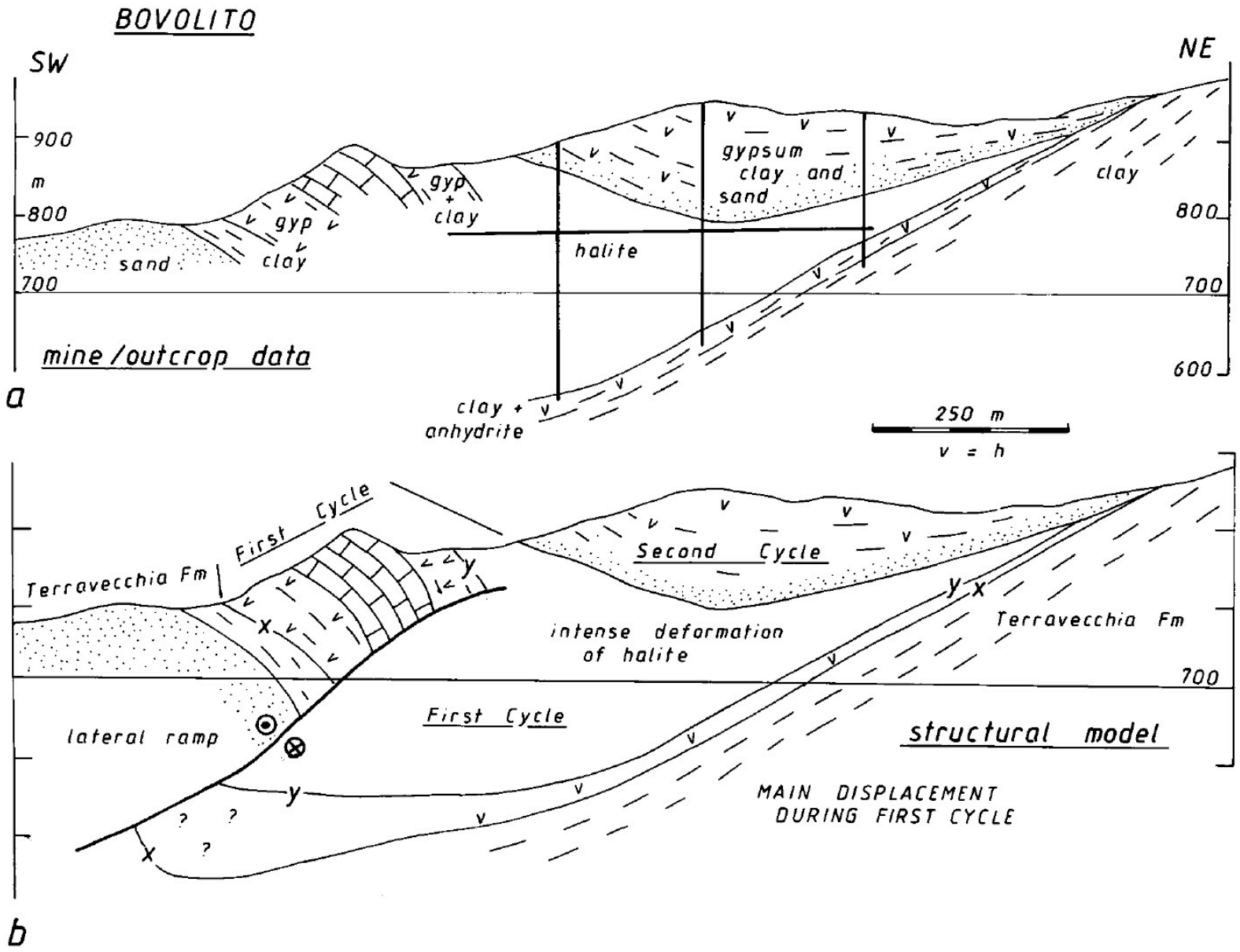

igure 8. Geology of the Bovolito basin (location on Fig. 2). (a) Profile of the basic data available from commercial exploitation of the t cycle halite. (b) Structural interpretation of Figure 8a. Key surfaces (x and y) are indicated to correlate with other parts of the

Butler et al 1995

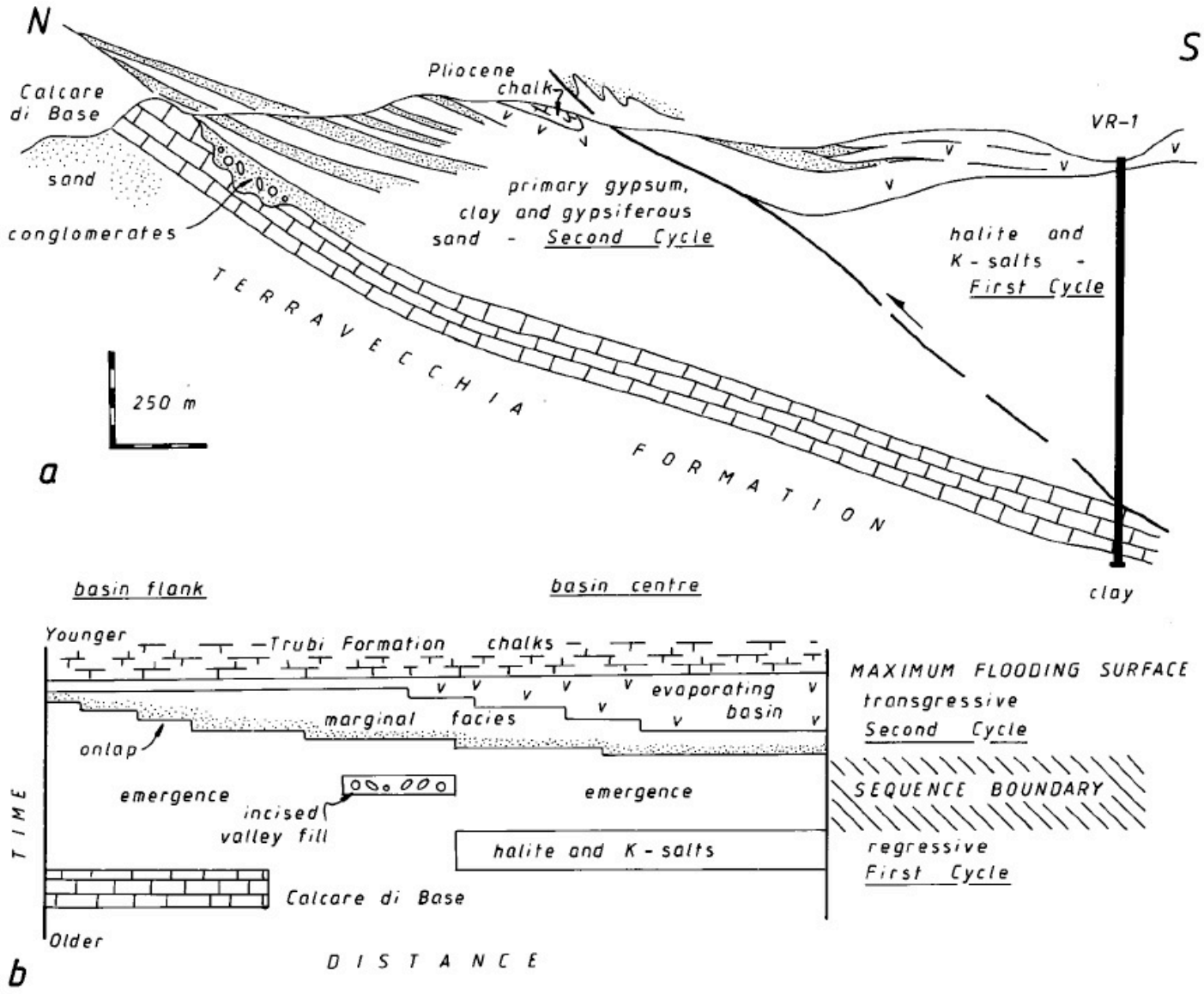

Figure 11. (a) True-scale structural section through the northern flank of the Corvillo basin (detail of Fig. 6), showing the relationship between first and second cycles within the Gessoso Solfifera Formation. Sands are stippled (gypsiferous for second cycle), while gypsiferous clays and selenite are indicated by v's. (b) Idealized chronostratigraphic model for the northern flank of the Corvillo basin, with relative time plotted against horizontal distance. At present the time scale is only relative. Work is underway to calibrate this using magnetostratigraphy.

Butler et al 1995

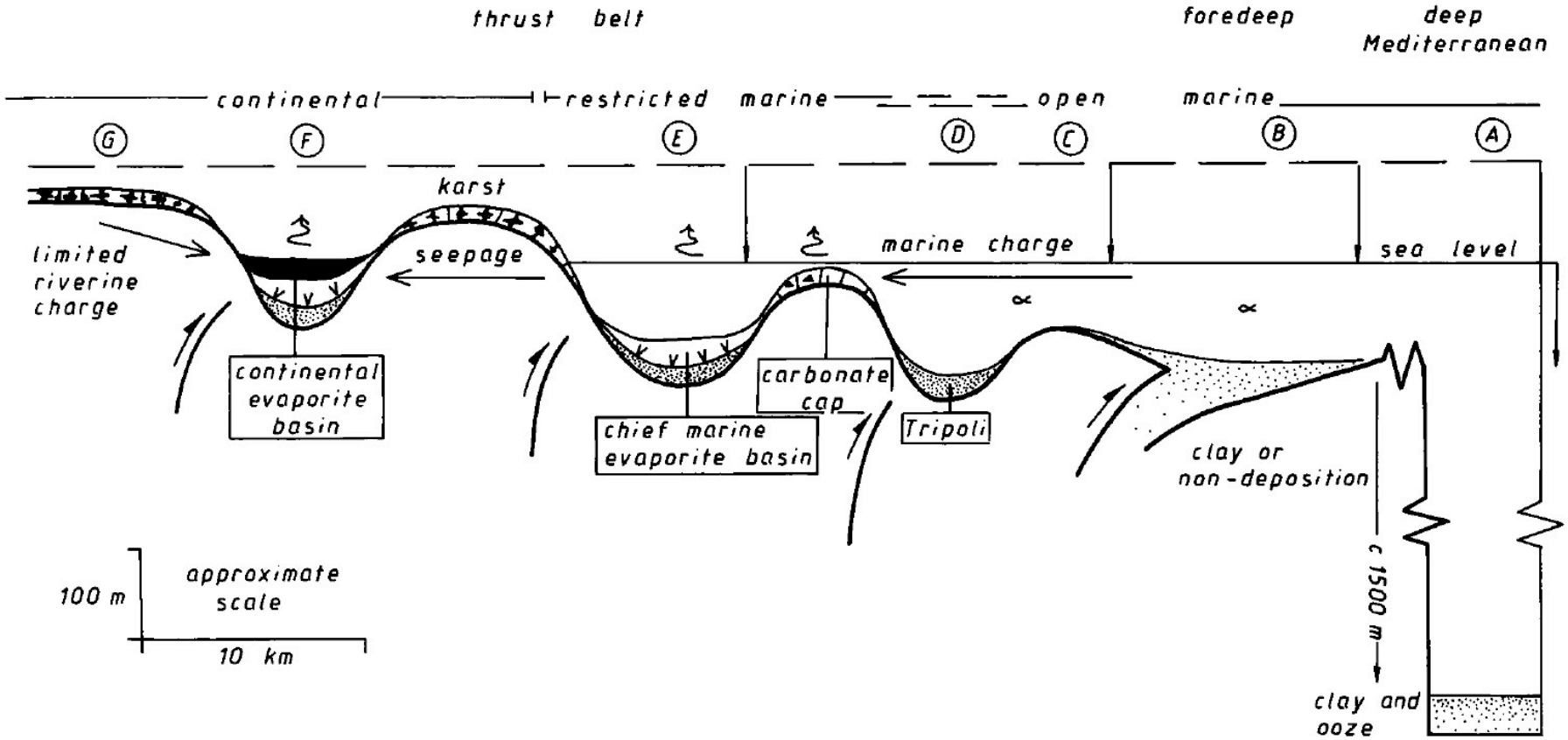

Figure 10. Regional model for evaporite stratigraphy across different thrust-top basins, illustrated schematically. At the instant shown, evaporitic drawdown has left one basin isolated from marine charge. The chief evaporitic basin is accumulating higher-order salts, with marine water concentrating across a shallow barrier. Ahead of this barrier the seawater is not sufficiently concentrated to precipitate evaporites, but restricted circulation allows diatomic laminites and torbas to accumulate in subbasins. Normal marine conditions persist in deep basin settings. Continued drawdown would lead to a progressive facies migration across the subbasins with all becoming emergent before salinity increases sufficiently for evaporite precipitation in the open marine environment. Locations A–G link this figure with the

Butler et al 1995

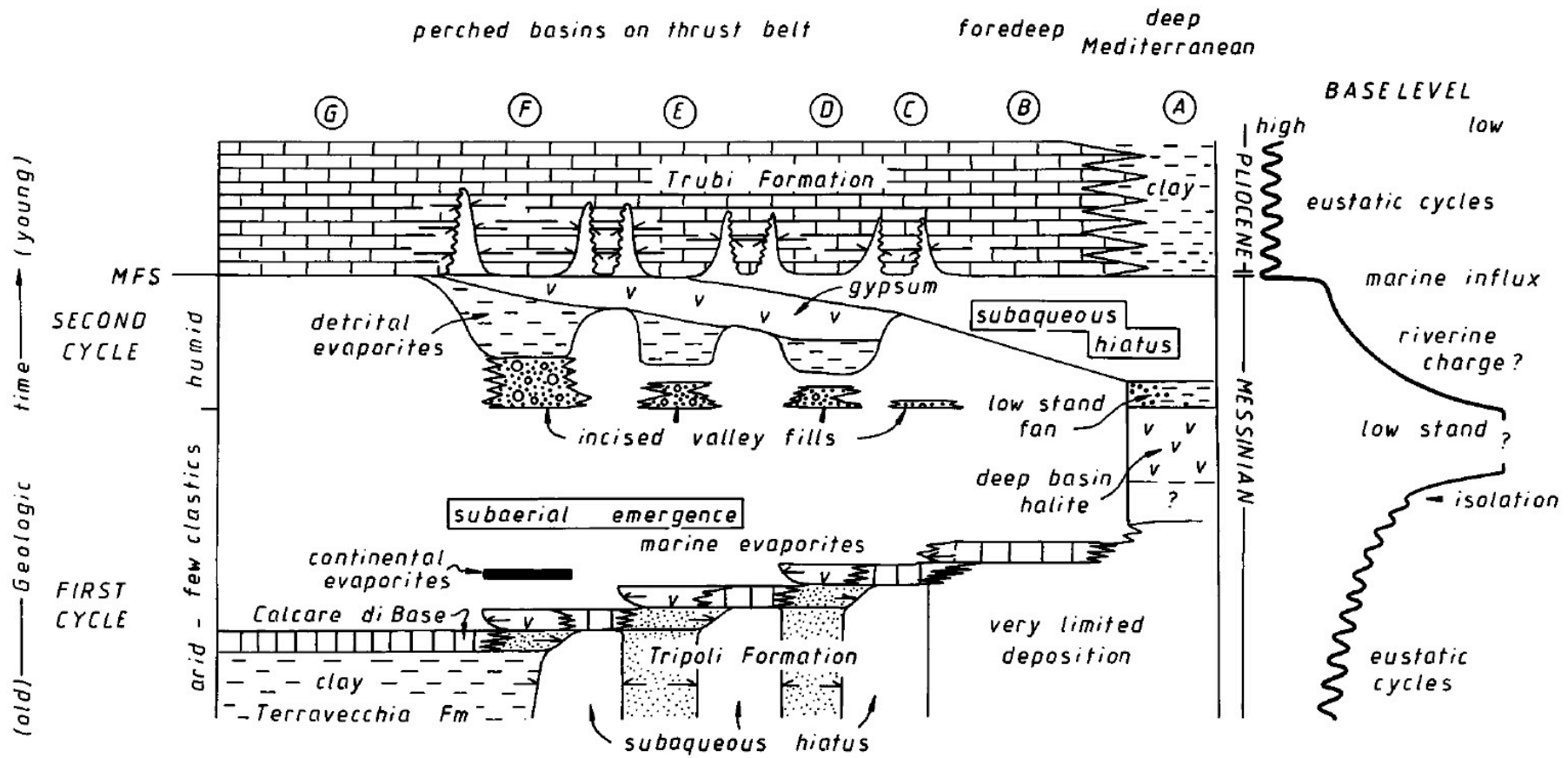

Figure 12. A relative chronostratigraphic model for Messinian and lower Pliocene deposits on Sicily and their correlation with abyssal depths of the Mediterranean. Time on the figure is unscaled and is awaiting future calibration against an absolute chronostratigraphy. This calibration will also provide a test of the model's prediction of diachroneity. The relative base-level fluctuations are schematic. Labelled sites A–G correlate with Figure 10. See text for further details.

Butler et al 1995

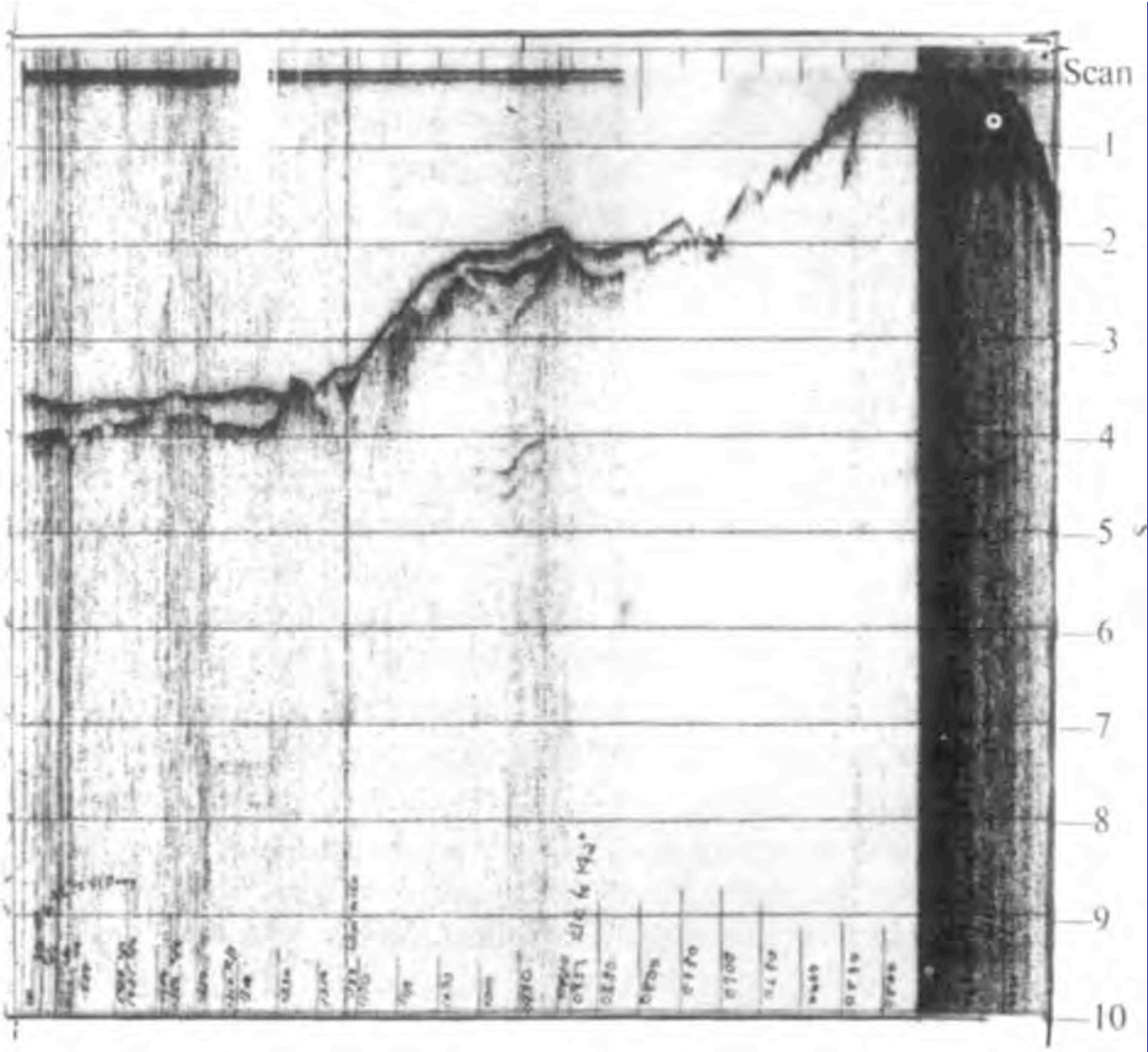

Fig. 1 The Mediterranean reflector. This strong reflector corresponds to the top of the Upper Miocene evaporite formation. The relief of the reflector conforms the bottom topography, suggesting that the evaporites were deposited in a basin similar in topography to that of the present Mediterranean.

NATURE VOL. 242 MARCH 23 1973

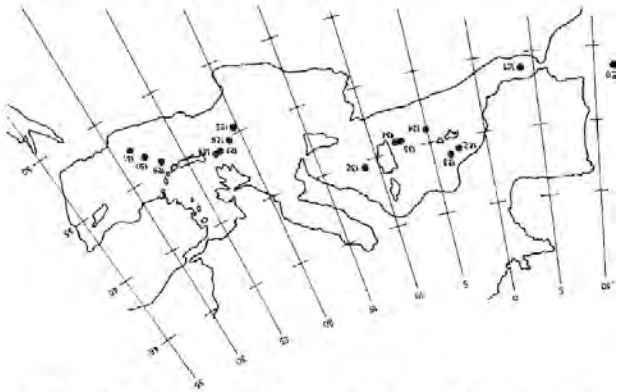

Fig. 2 Drill sites of Leg XIII of the Deep Sea Drilling Project.

Hsu et al 1973

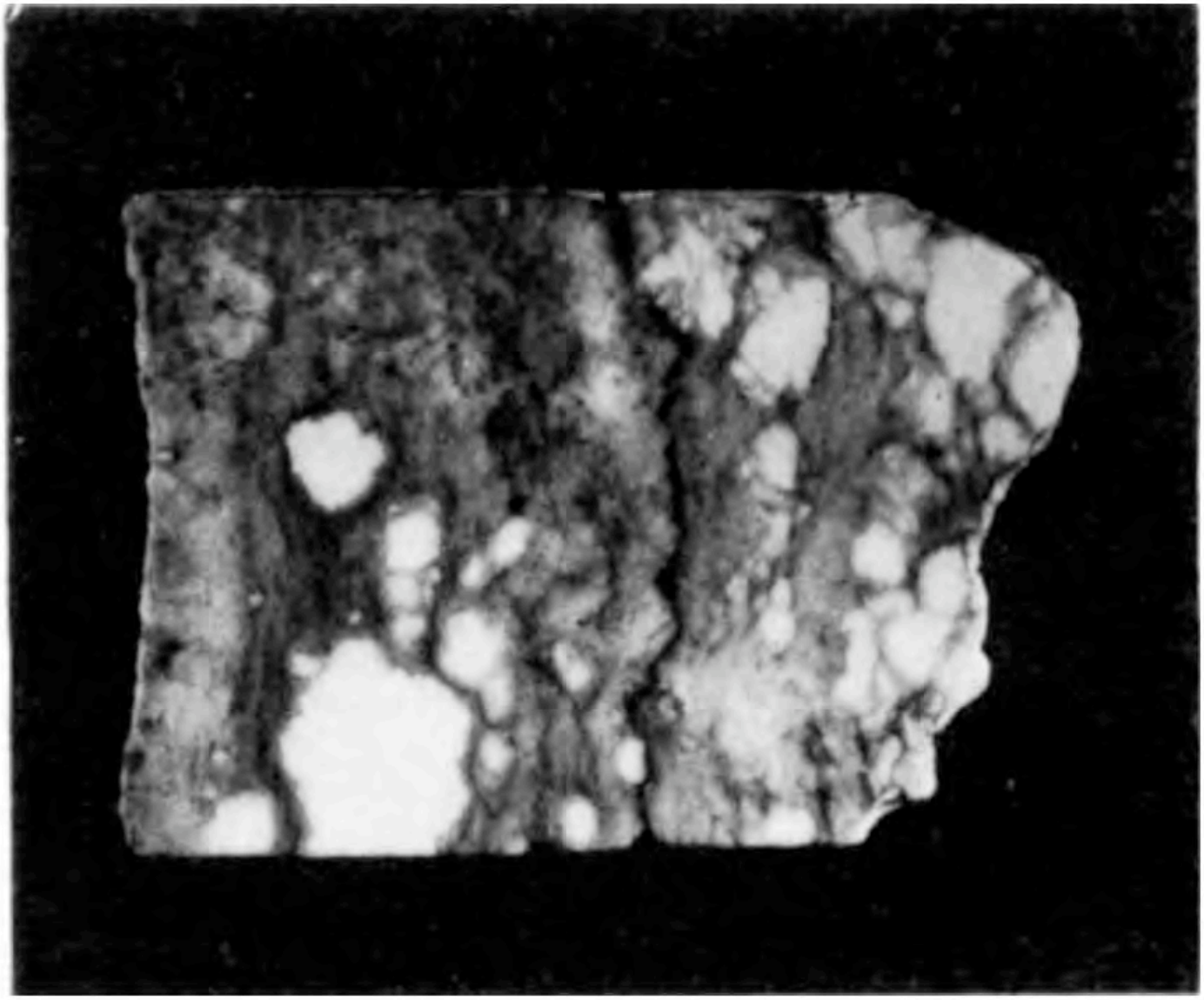

Fig. 3 Nodular and "chicken wire" anhydrite, characteristic precipitates from ground waters under hot and arid coastal flats.

Hsu et al 1973

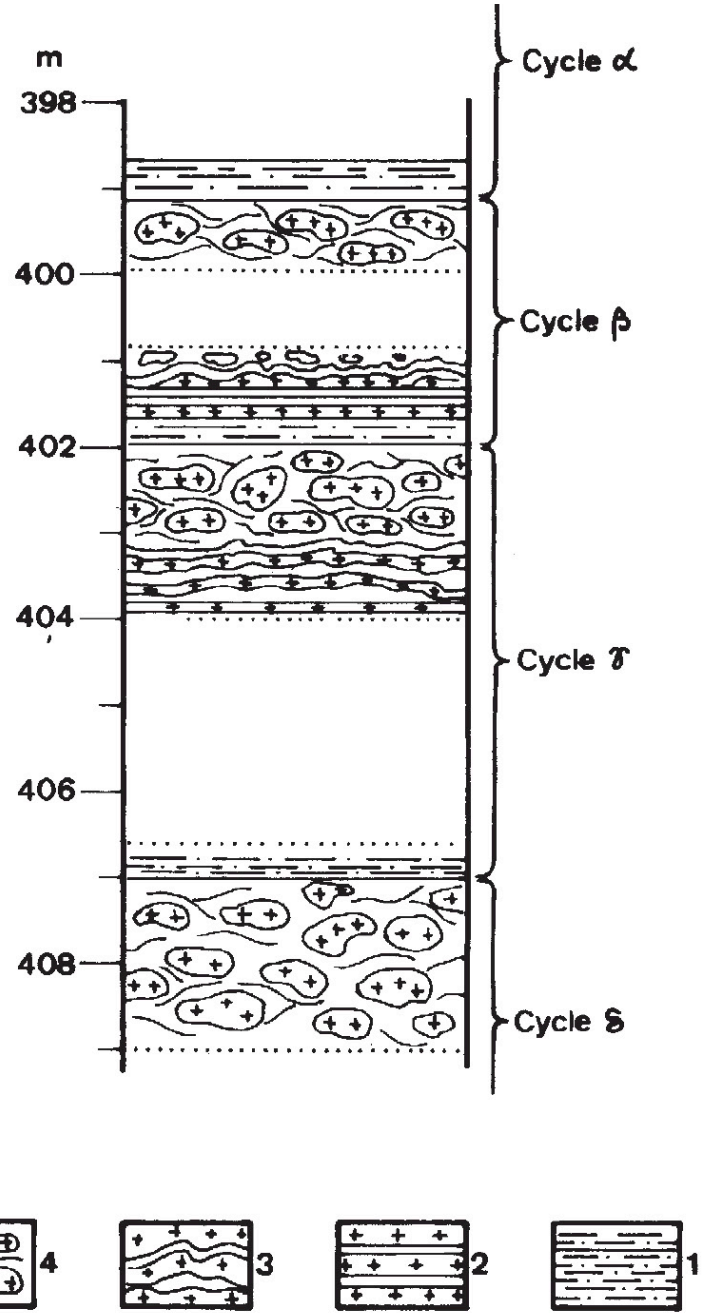

Fig. 4 Schematic diagram of desiccation cycles in hole 124. 1, Laminated carbonates; 2, interlaminated dolomite and anhydrite; 3, stromatolitic deposits; 4, nodular anhydrite.

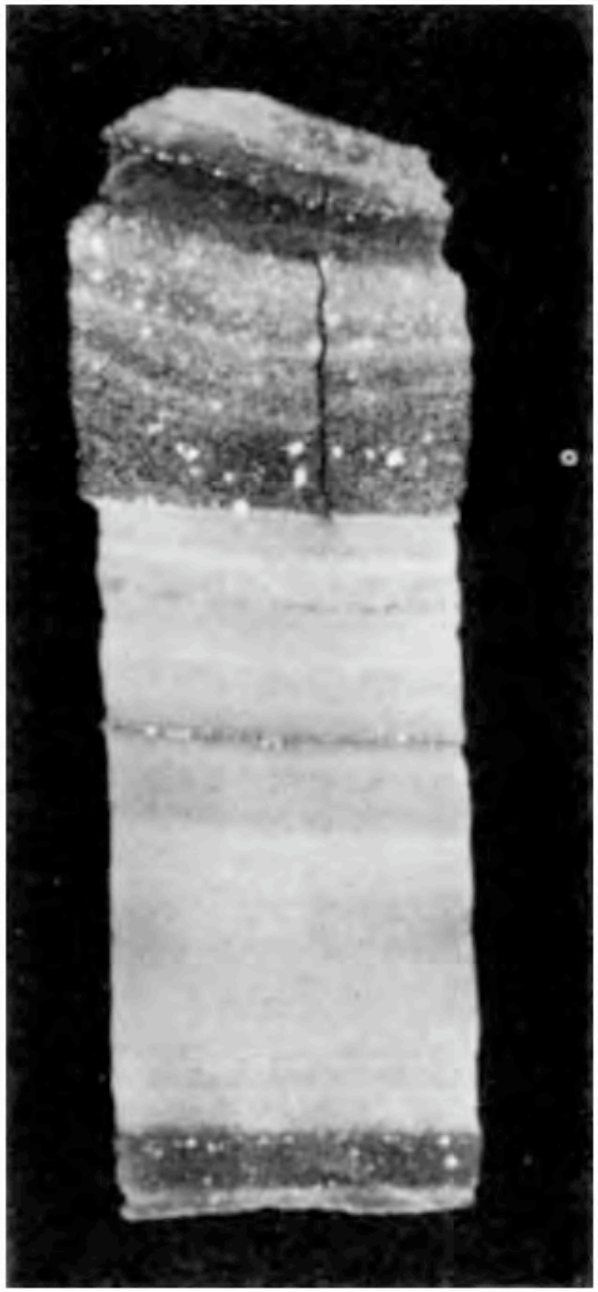

Fig. 5 Halite core from site 134.

Hsu et al 1973

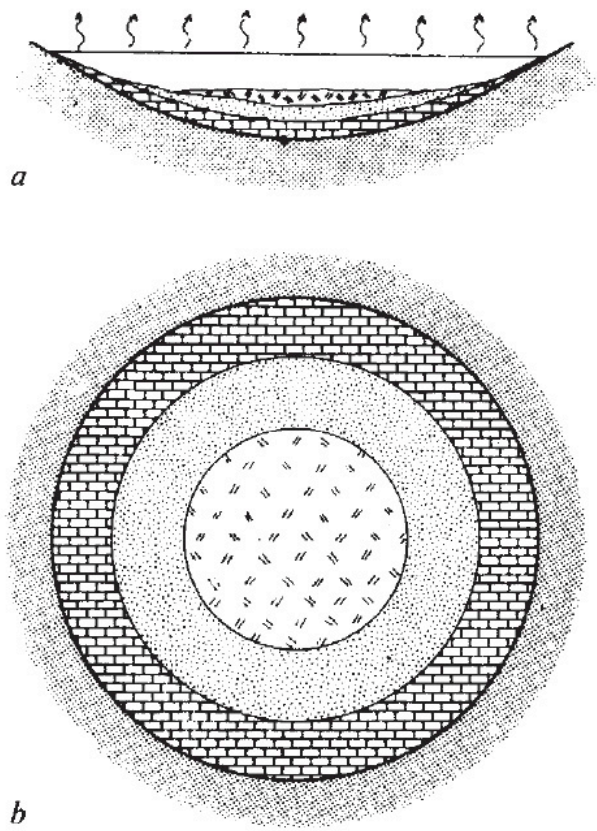

Fig. 7 Idealized bull's eye pattern of evaporite distribution typical of isolated basins. *a*, Cross-section; *b*, map.

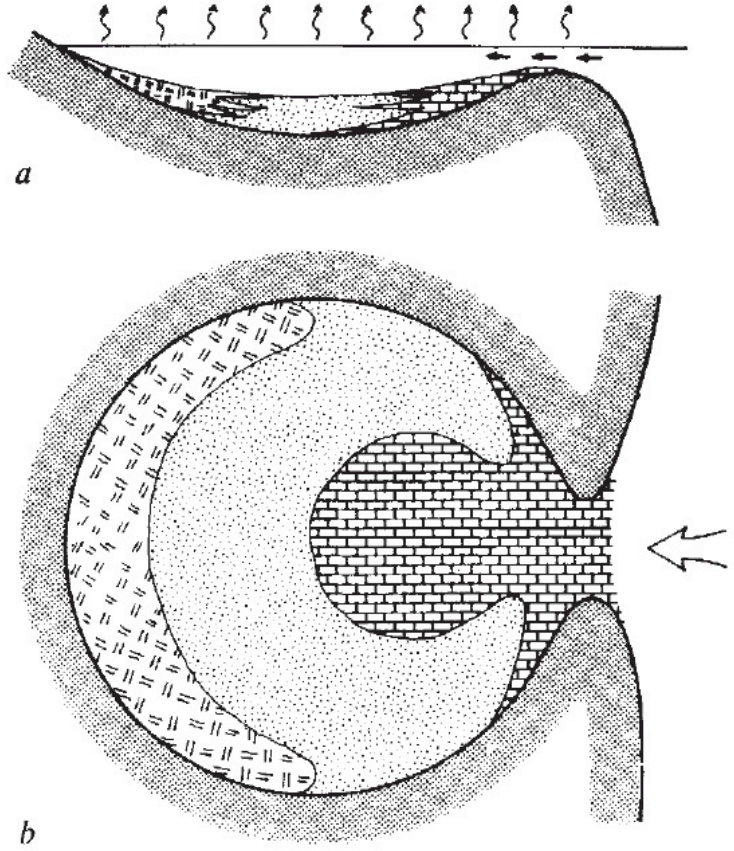

Fig. 8 Idealized tear drop pattern of evaporite distribution typical of partially restricted basins. *a*, Cross-section; *b*, map.

Hsu et al 1973

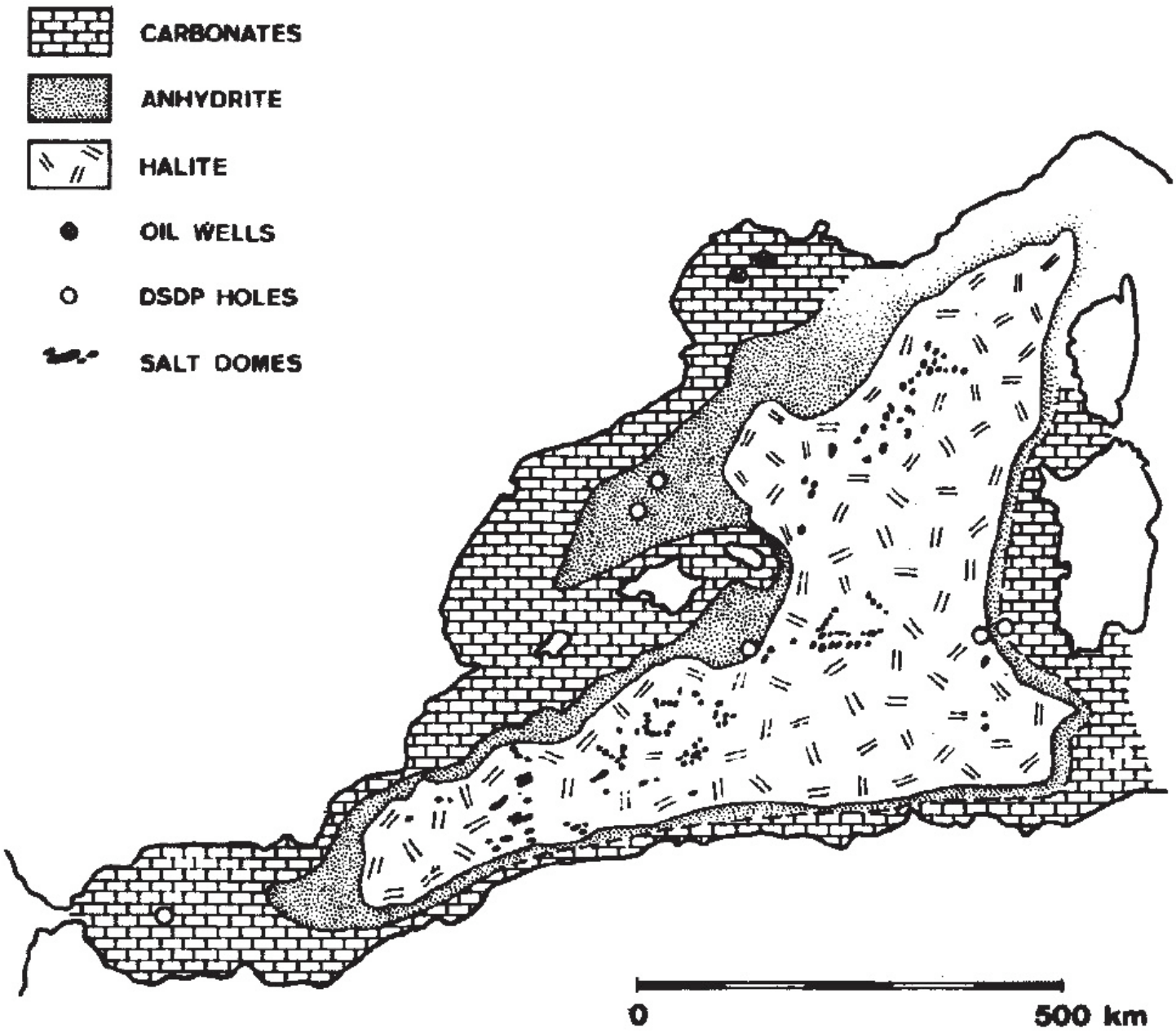

Fig. 9 Probable distribution of evaporites in the western Mediterranean Balearic Basin.

Hsu et al 1973

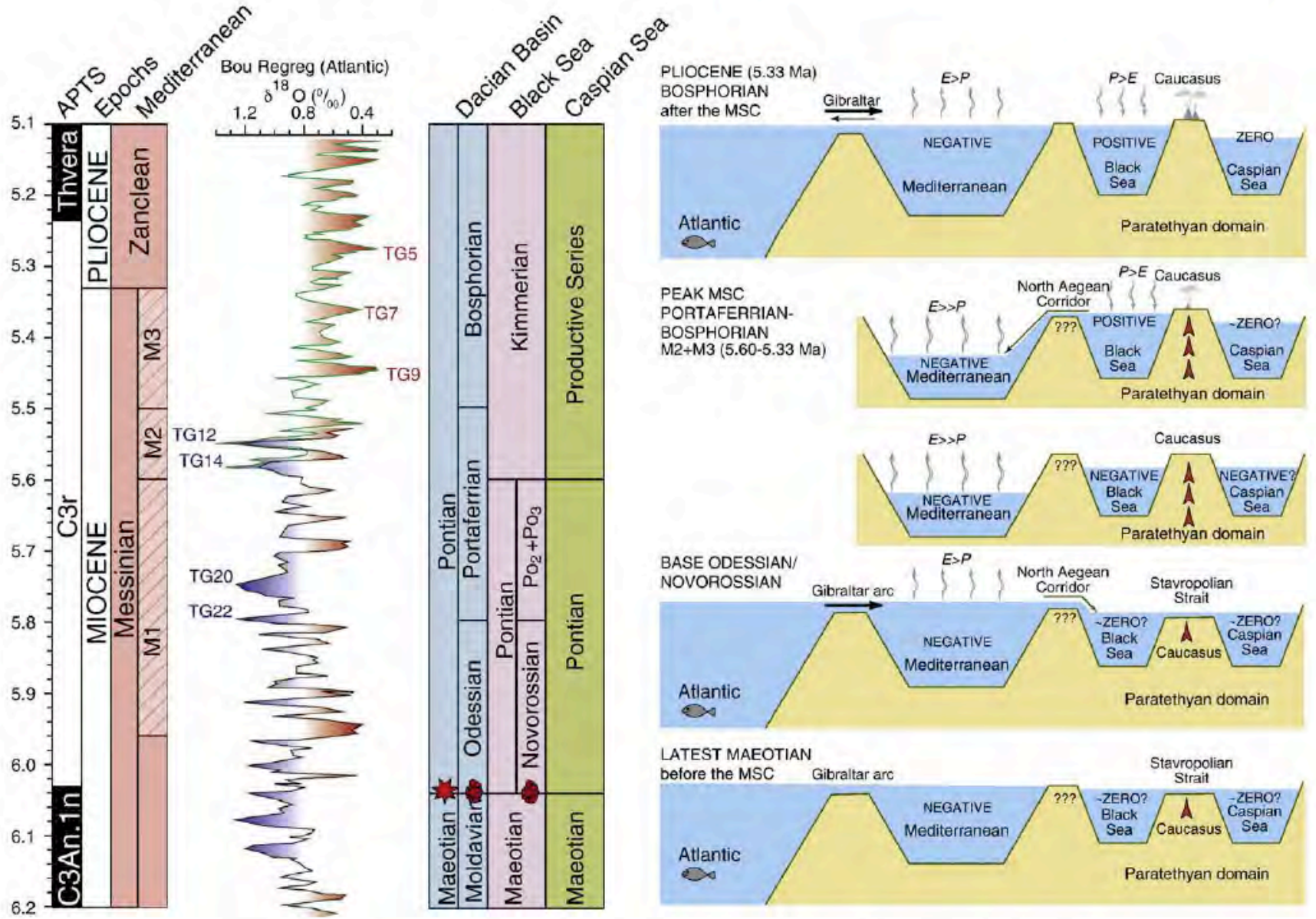

Fig. 6. A new chronology for the different local and regional stages of the Paratethys allows detailed correlations to the GTS, the Mediterranean event stratigraphy during the Messinian Salinity Crisis (M1–M3) (Krijgsman et al., 1999; Roveri et al., 2008) and to the oxygen isotope curves of the Atlantic margin of Morocco (Hilgen et al., 2007). Red star/foraminifer indicates influx of marine nannofossils (Marunteanu and Papaianopol, 1998)/foraminifera (see Fig. 4). Schematic cross-sections show the changes in connectivity and the phases of basin isolation of the Paratethys and Mediterranean during the Messinian Salinity Crisis.

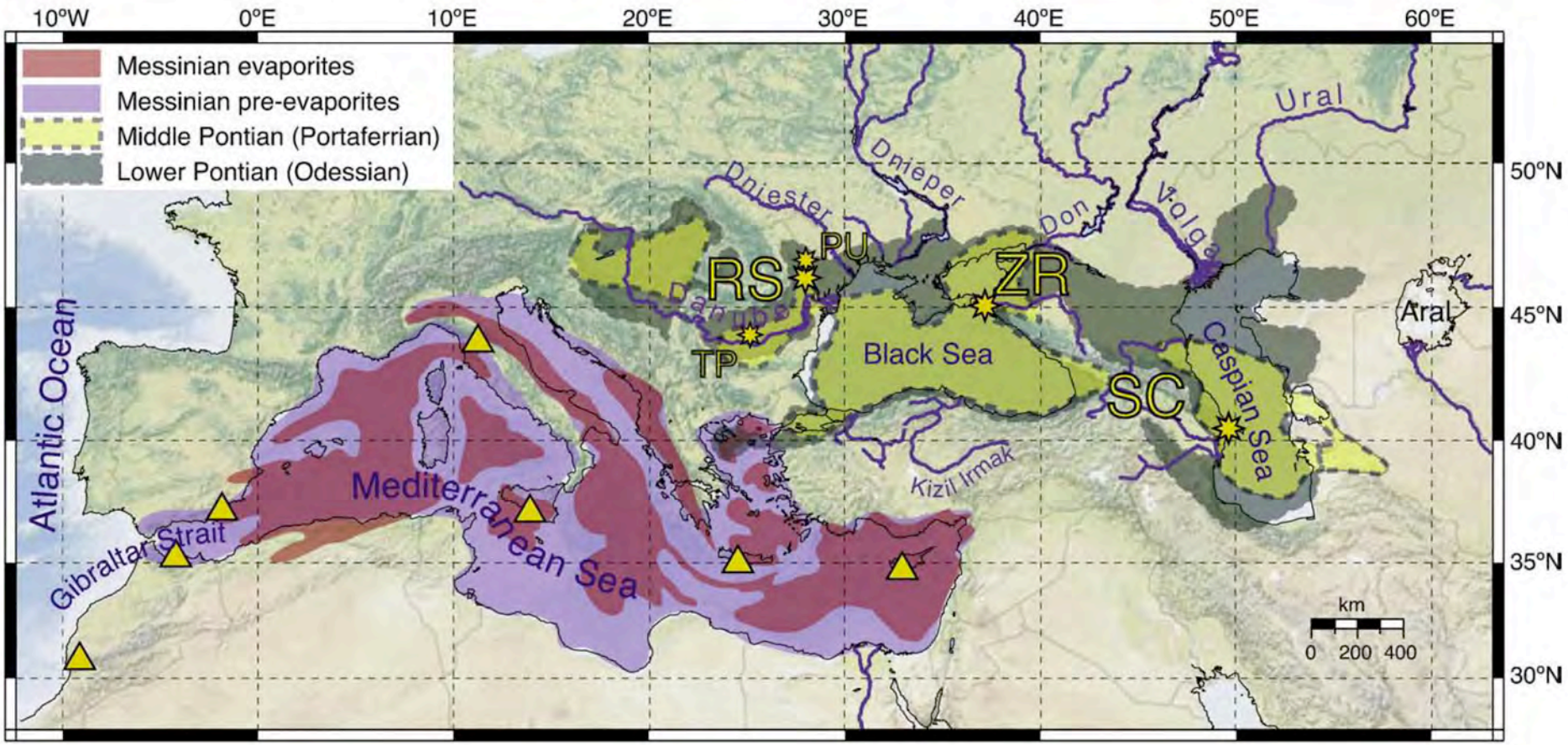

Fig. 1. Paleogeographic map of the Mediterranean and Paratethys during the Messinian Salinity Crisis interval. Stars indicate locations of the sections and research areas. In the Dacian Basin, RS and PU = Râmnicu Sarat and Putna sections are located in the east Carpathian foredeep and TP = Topolog region is in the south Carpathian foredeep. In the Black Sea basin, ZR = Zheleznyi Rog section is located on the Taman Peninsula of the Russian Black Sea margin; SC = South Caspian Basin — Azerbaijan. Triangles locate astronomically dated

Krijgsman et al 2010 Messinian Salinity Crisis Paleogeography